Available online at www.sciencedirect.com

SciVerse ScienceDirect

Ceramics International 39 (2013) 539–546

CERAMICS INTERNATIONAL

www.elsevier.com/locate/ceramint

A novel approach on the preparation of biphasic calcium phosphate bioceramics under physiological conditions. The effect of the starting material

Martha Aslanidou[a], Tiverios Vaimakis[a,*], Anastasios Mitsionis[a], Christos Trapalis[b]

[a]*Chemistry Department, University of Ioannina, P.O. Box 1186, 45110 Ioannina, Greece*
[b]*Department of Material Science, National Research Center, Demokritos, 15310 Ag. Paraskevi, Athens, Greece*

Received 26 April 2012; received in revised form 20 June 2012; accepted 20 June 2012
Available online 29 June 2012

Abstract

Biphasic Calcium Phosphate (BCP) bioceramics were prepared in physiological pH. Salts of Calcium and Phosphate with initial molar ratio of Ca/P=1.67, similar to Hydroxyapatite (HA) stoichiometry, were precipitated by the addition of NH_4HCO_3 1 M. XRD results of the as prepared materials show that high crystalline $CaHPO_4 \cdot 2H_2O$ (DCPD) was produced, resulting a decrease of the initial Ca/P ratio. However ageing of the slurry under continuous stirring for 1 and 2 days time, lead to the gradual hydrolysis of dicalcium phosphate dihydrate (DCPD) to low crystalline HA producing biphasic HA/DCPD particles. Ageing time affects also the morphology of the materials. SEM images show that the initial lath-like DCPD particles with HA during the ageing were transformed firstly into bigger particles and flake like particles afterwards. The above mentioned are in accordance to the results of TG/DTA analysis. The morphology and the phase composition of the yielding materials depend on the initial concentration of HCO_3^- and ageing time. Hydrolysis of NH_4HCO_3, affects the precipitation of both Ca^{2+} and PO_4^{3-} on the starting material, under physiological pH and thus has to be manipulated properly in order to achieve the desirable results in a possible hard tissue evaluation of in vitro bioactivity.

Keywords: Biphasic calcium phosphate; DCPD; Hydroxyapatite; Hydrolysis–precipitation

1. Introduction

Since the past three decades the applications of bioceramics in many areas of our life has been multiplied. Nowadays calcium phosphate bioceramics have been used for medical purposes as heart pumps, implants, drug delivery systems and biological matrixes. Their biocompatibility and chemical similarity to the natural human hard tissue led to the utilization of such materials as artificial implants. However there are several problems we have to overcome in order to achieve best results. Therefore many efforts have been made in order to improve the mechanical properties and the material performance at prostheses in the human body [1–5]. Most of the human tissue fluids have pH values between 7.2 and 7.5 calibrated through the physiological ionization of carbonic acid (H_2CO_3) and phosphoric acid (H_3PO_4). During this procedure the conjugate base of carbonic acid, bicarbonate ion (HCO_3^-) is produced which leads to the formation of carbonated hydroxyapatite in the human hard tissues. Carbonated Hydroxyapatite (cHA) is the major content of the human hard tissue, providing both teeth and bones flexibility, stability and functionality [6]. In addition, porosity of biomaterial scaffold has been noted to play an important role in vitro mechanical properties as well as in vivo resorption and new bone ingrowth.

The most important biological apatite used as implant is hydroxyapatite (HA, $Ca_{10}(PO_4)_6(OH)_2$). HA's chemical similarity, non-toxicity and bonding capability to the natural bone are considered to be its great advantages. HA is the most insoluble and stable material above all orthophosphoric calcium salts [7,8]. Other calcium phosphates applied in the same area are: Dicalcium phosphate dihydrate (Brushite, DCPD, $CaHPO_4 \cdot 2H_2O$) which is an intermediate of

*Corresponding author.
E-mail address: tvaimak@cc.uoi.gr (T. Vaimakis).

0272-8842/$36.00
http://dx.doi.org/10.1016/j.ceramint.2012.06.060

HA precipitation and can be used as dentine modifier though fluorine ions, Tricalcium phosphate (TCP, $Ca_3(PO_4)_2$) which can be found in an α-TCP or β-TCP form and is used as bone ceramic substitute, carbonated Hydroxyapatite (cHA) and Octacalcium phosphate ($Ca_8H_2(PO_4)_6 \cdot 5H_2O$, OCP). Each one of the above mentioned materials has its own properties that can be used for different purposes such as active hardening agents, bioresorbables surface modifiers, coatings and/or for biomedical purposes [9–15]. Currently biphasic calcium phosphate (BCP) materials represent the most promising and best alternative for bone reconstructions. The chemical and physical properties of BCPs are affected from the Ca/P ratio, pH, temperature, and duration of the sintering process, and consequently could lead to different tissue responses [16,17]. Depending on their applications BCPs need to be highly resorbable (i.e. in the case of alveolar ridge augmentation) or highly stable (i.e. in the case of implants used as coatings).

The combination of a balanced ratio between different kinds of calcium phosphate materials could produce new BCP materials with the desirable dissolution rate and different mechanical properties, for example a combination of a more stable material (HA) with a more soluble one (β-TCP) [18]. The bioreactivity of BCPs and consequently their degradability can be manipulated through phase composition, porosity, proliferation, leading to the formation of more biocompatible, osteoconductive and in some cases, osteoinductive ceramics, which can favor increased bone formation [17,19–21].

BCPs can be prepared through many different procedures and starting materials. Spassova et al. [22] used red marine algae to produce HA/b-TCP composites of different HA/b-TCP ratios by hydrothermal process. By varying the Mg addition and the parameters of the hydrothermal process, the concentration ratio of HA and b-TCP was controlled to obtain biphasic composites with b-TCP content up to 95 wt%. Emadi et al. [23] synthesized biphasic composites at room temperature by treating calcined bovine bone with P_2O_5 solution. The crystalline phase composition could be controlled by reaction time. Porous BCPs prepared by Spassova were granular and had porosity in the range of 1–10 mm, which limits their application for bone repair. Xenografts, such as bovine bone-based BCPs have serious shortcomings including a variation in properties and quality, in addition to a greater risk of disease transmission. Natural cuttlefish bone was also successfully converted to porous BCP scaffolds with various HA and b-TCP compositions by a simple solution reaction followed by sintering at high temperatures [24].

The application of HA, has already been proposed as modulating factor in order to extend DCPD cement setting. Alge et al. [25] found that the setting reaction proceeded vigorously for cements prepared with poorly crystalline HA, also they found evidence that the conversion of DCPD to HA occurs rapidly in vitro and thus reduces cement resorbability. This finding could have considerable implications for the clinical utility of these cements, as well as other HA based DCPD cement formulations.

The scope of this work is to investigate the preparation of biphasic phosphate materials at physiological pH in vitro from an acidic solution containing an initial amount of calcium and phosphate similar to the theoretical ratio of HA stoichiometry (Ca/P = 1.67). BCP materials were prepared by neutralization using NH_4HCO_3. The bicarbonate ions produced during the procedure, along with phosphate ions, are considered to act as the natural pH buffer of the human body fluids. As the pH value steadily increases, hydrolysis processes enhance the formation of different phosphate species in the solution.

A pH standard chart (available in the Sigma Chemical Inc. catalog) as a function of temperature was used to estimate pH at 36.6 °C from a pH titrated at room temperature. Thus, a pH of 7.5 measured at 25 °C will correspond to pH 7.24 at 36.6 °C. According to Hsu and Abbo [26] the importance of this biological buffer in the biological calcification process lies in the unlimited supply of CO_2 and the rapidity of this buffer in reversibly attaining alkalinity and acidity of extracellular fluids. This unique property may provide an important factor in order to initiate or prevent unwanted calcification and could be also a preview of the regeneration mechanism which could be adopted by the body in order to facilitate the repair of a possible bone fracture under physiological conditions in the early stages. Ageing time of one and two days was chosen in order to simulate the initial in vitro osteoclast (OC) attachment period on natural dentine or bioceramics via cell adhesion or osteoblastic (OB) bone deposition under physiological conditions [27]. Ramaswamy et al. [27] showed that human OCs can attach and degrade calcium phosphate materials according to their surface composition, solubility and morphology. However they did not investigate the interaction of both HCO_3^- and phosphate species which can dictate the OCs adhesion on materials at the early stages.

The materials' phase composition was also modified via calcination in order to obtain products with different properties such as morphology, chemical composition and solubility. Calcination temperature of 900 °C was chosen due to the thermal and structural stability properties of the as prepared materials. Sintered HA and β-TCP ceramics can also bond directly with host bone [28–30]. Their apatite-formation ability mainly depends on their crystallinity and sintering properties. Fully sintered HA bulk ceramics are difficult to induce bone-apatite formation and sintered β-TCP ceramics exhibit poor ability of inducing apatite formation; [31–33] however, HA particles can induce apatite formation [34]. The obtained materials were studied using Thermal Analysis, XRD and FT-IR techniques while the textural properties were investigated by SEM technique.

2. Materials and methods

The reagents that have been used were $CaCl_2 \cdot 2H_2O$ (Fluka, Assay (KT) 99%), $Ca(H_2PO_4)_2 \cdot H_2O$ (Riedel-de

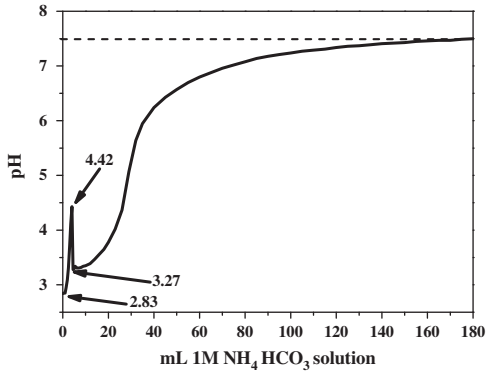

Fig. 1. Neutralization of the Ca/P solution using 1 M NH_4HCO_3.

Han, Assay 88%), NH_4HCO_3 (FERAK) and distilled water.

A solution of 0.025 M of $Ca(H_2PO_4)_2 \cdot H_2O$ and 0.0584 M $CaCl_2 \cdot 2H_2O$ was prepared. The molar ratio in the acquired solution was Ca/P = 1.67 and the pH value equal to 2.83. In a glass beaker was placed 200 ml of the solution and under continuous stirring small portions (0.5 mL) of a 1 M NH_4HCO_3 solution were added. After each adding the mixture was stirred until its pH value was steadied. The addition of NH_4HCO_3 solution was continued until the pH of the mixture increased from 2.83 to 7.50. The produced white slurries were filtered through Milipore filters (0.8 μm pore size), washed with distilled water and acetone instantly, and dried at 90 °C for 1 day. The sample was named ph75d0, indicating the yielding precipitation pH (7.5) and the aging time (0 day), correspondingly. The procedure was repeated and the slurries were aged, under continuous stirring, for 1 and 2 days. The samples were named ph75d1 and ph75d2 for aging time (a.t.) 1 and 2 days, correspondingly. Each one of the prepared samples was calcined at 900 °C with heating rate of 5 °C/min for 3 h. The final materials obtained, have sample names cph75d0 (a.t. = 0d), cph75d1 (a.t. = 1d), cph75d2 (a.t. = 2d), correspondingly.

The identification of the crystal phases in the obtained products was carried out by the X-ray diffraction (XRD) technique, using a Brüker P8 Advance apparatus, with a 2θ range of 20°–60° in steps of 0.02° and the identification of the patterns was made by the cards of the International Centre for Diffraction Data (ICDD). FT-IR was performed using a spectrophotometer (Model Spectrum RX I FT-IR, Perkin-Elmer). The KBr disk technique was used with ~2 mg of powder in ~200 mg of spectroscopic-grade KBr (Merck), which had been dried at 100 °C. Infrared spectra were recorded in the 4000–400 cm^{-1} region.

The texture of the solids were examined by scanning electron microscopy (SEM), using a JEOL JSM-6300 instrument. Simultaneously TG/DTA (thermogravimetry/differential thermal analysis) measurements were carried out by a STA 449C (Netzch-Gerätebau, GmbH, Germany) thermal analyzer. The heating range was from room temperature up to 1400 °C, with a heating rate of 10 °C min^{-1} under synthetic air flow rate of 30 cm^3 min^{-1}. Alumina (Al_2O_3) powder was used as reference.

The calcium and phosphate content of the as prepared samples were carried out using the ICP-AES technique using a Model Optima 3000, Perkin Elmer, (Norwalk, CT) spectrometer as described in our previous work [35]. Ca/P content was determined using calibration curves. Calibration standards were made using standard solutions (Merck, Darnstadt, GER) and were formulated to be matrix matched to all samples.

3. Results and discussion

Fig. 1 shows the neutralization process that takes place after the addition of 1 M NH_4HCO_3 solution in the initial Ca/P solution. After the addition of 4 mL of 1 M NH_4HCO_3 solution there is a rapid increase of pH value form the initial 2.83 to 4.42 attributed to the production of $H_2PO_4^-$ ions (reaction 1). By adding a small portion of 1 M NH_4HCO_3 solution the HPO_4^{2-} ions react with Ca^{2+} ions forming dicalcium phosphate which precipitates (reaction 2) as dihydrate salt (DCPD). The formation of DCPD solid leads to a dramatically decrease of pH value from 4.42 to 3.27. From this point the pH increase has a sigmoid shape until the yielding pH 7.5, with inflection point pH ~5.

$$H_2PO_4^- + HCO_3^- \rightarrow HPO_4^{2-} + H_2O + CO_2\uparrow \quad (1)$$

$$Ca^{2+} + HPO_4^{2-} + 2H_2O \rightarrow CaHPO_4 \cdot 2H_2O\downarrow \quad (2)$$

In order to investigate the exact way phosphate precipitates under different pH values, we calculated the equilibrium concentrations of phosphate species, using the equilibrium constants (Table 1 and Fig. 2). As it can be seen at pH ~4.6 the main form in the solution is $H_2PO_4^-$. From this point the concentration of HPO_4^{2-} species increases partially until yielding pH of 9.6. pH 7.2 signifies the point in which the amount of $H_2PO_4^-$ and HPO_4^{2-} is about equal in the solution. This pH value corresponds to the physiological pH of the aqueous humor of the human body. Slightly higher values of pH correspond to blood (7.25–7.4) and cerebrospinal fluid (7.35). Calcium phosphate materials can be soluble in the body fluids and their mobility depends on the pH value. Since calcium phosphate materials are highly bioactive, they can be resorbed by the human body through two distinguished mechanisms (1) active resorption regulated by living cells (i.e. macrophages, osteoclasts) and/or (2) passive resorption via chemical dissolution or hydrolysis in the body

Table 1
Phosphate equilibrium constants.

Equilibrium	K_a	pK_a
$H_3PO_4 \leftrightarrow H_2PO_4^- + H^+$	7.6×10^{-3}	2.12
$H_2PO_4^- \leftrightarrow HPO_4^{2-} + H^+$	6.2×10^{-8}	7.21
$HPO_4^{2-} \leftrightarrow PO_4^{3-} + H^+$	4.2×10^{-13}	12.38

fluids [36]. Brushite is soluble in body fluids, thus brushite cements are mainly resorbed by passive mechanism [37,38] while apatites being less soluble, cause apatite cements to be mostly resorbed by the active mechanism [39,40]. Chemical composition and solubility of the substrate surface morphology contributes significantly to cellular behavior such as Osteoclast (OC) attachment [27,41].

Fig. 3a and b present the XRD patterns of samples prepared in pH 7.5 before and after calcination correspondingly, after ageing of 0, 1 and 2 day-time. Sample ph75d0, prepared without ageing, is biphasic and seems to be consisted of DCPD and HA (ICDD card 72-1240 and ICDD card 84-1998 correspondingly). The ageing of the slurry gave different XRD patterns. Samples ph75d1 and ph75d2 are consisted of low crystalline HA while the DCPD peaks are decreasing in sample ph75d1 and are absent in sample ph75d2. The XRD pattern of sample cph75d0, prepared after calcinations at 900 °C, shows the presence of biphasic materials β-TCP/CPP. The formation of β-TCP (ICDD card, 70-2065) and calcium pyrophosphate (CPP/$Ca_2(P_2O_7)$ (ICDD card, 81-2257) can be explained by the thermal transformation of both DCPD and HA according to reactions 3 and 4.

$$2CaHPO_4 \cdot 2H_2O \rightarrow Ca_2P_2O_7 + 5H_2O \quad (3)$$

$$Ca_{10}(PO_4)6(OH)_2 + Ca_2P_2O_7 \rightarrow 4Ca_3(PO_4)_2 + H_2O \quad (4)$$

Sample cph75d1, according to the XRD pattern, is consisted of high crystalline β-TCP and traces of CPP. The later could be explained by the decomposition of the calcium-deficient hydroxyapatite observed in the corresponding uncalcined sample (ph75d1). Ca-deficient HA can partially transform to CPP at about 500 °C (reaction 5).

$$Ca_{10-x}(HPO_4)x(PO_4)_{6-x}(OH)_{2-x} \rightarrow Ca_{10-2x}(PO_4)_{6-x}(OH)_{2-x}x/2Ca_2P_2O_7 + x/2H_2O \quad (5)$$

If the amount of CPP is high enough then the main product of the reaction 4 is β-TCP. The production of calcium deficient HA in sample ph75d1 is also pH dependable since the pH value also favors the production of HPO_4^{2-} species. Sample cph75d2, on the contrary, is consisted of pure HA with higher crystallinity compared to the non-calcined sample ph75d2. A crystalline phase with apatitic structural characteristics is most likely to be less soluble in the acidic environment where OCs are attached while could also lead to fastest rate of bone induction [27,42].

Fig. 4 depicts the FT-IR spectra of the samples prepared with pH value of 7.5 at different ageing times. The FT-IR spectrum of pH75d0 is in accordance to the XRD results. The spectrum shows the major absorbance peaks of both DCPD and HA. The P–O vibration of the HPO_4^{2-} group is appeared at 1649 cm^{-1}, while the stretching vibrations of O–P–O at the range between 1218 and 874 cm^{-1}. The double peaks at the ranges between 3539 and 3484 cm^{-1} and between 3162 and 3158 cm^{-1} are attributed to the two different types of crystalline water molecules. The peaks at 790 and 662 $cm^{-1}$are also attributed to the crystalline water. The O–H vibrations of the POH group are appeared

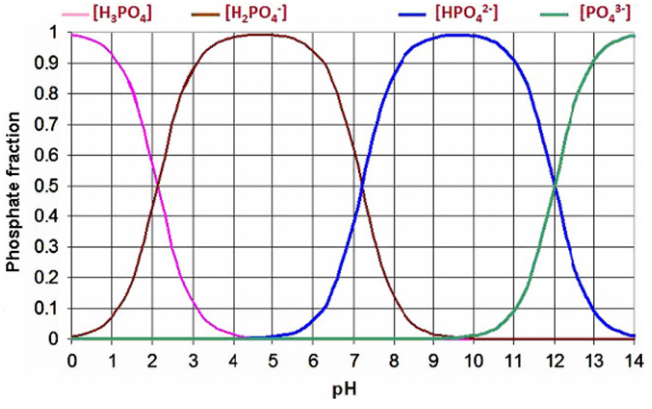

Fig. 2. Phosphate species transformation versus pH.

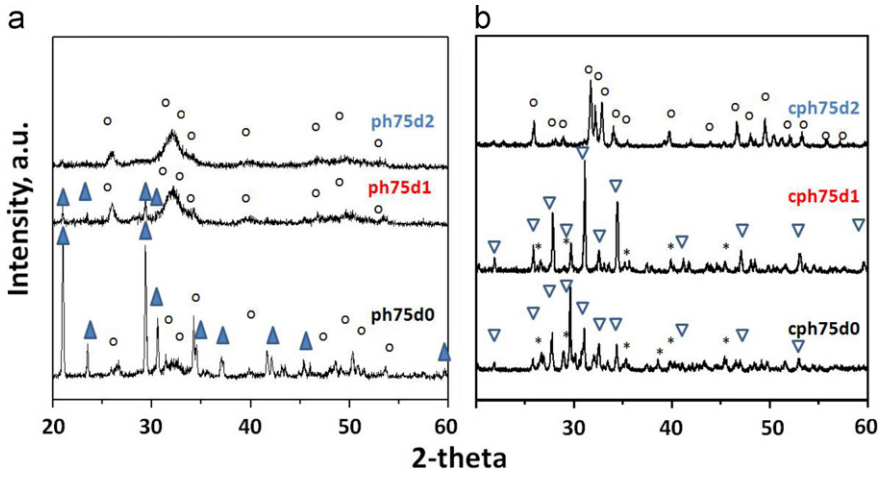

Fig. 3. XRD patterns of samples prepared in pH 7.5 without calcination (a) and after calcination(b). (o) denotes HA, (*) denotes CPP, (△) denotes β-TCP and (▲) denotes DCPD peaks.

at 2927, 2370, 2270 and 2121 cm^{-1}. The FT-IR spectra of samples pH75d1 and pH75d2, are more similar with the HA one. The pH75d1 has the vibrations 469, 568, 603, 959 and 1030 cm^{-1} of PO_4^{3-} group, as well as, the vibrations at 869 cm^{-1} and 873 cm^{-1} of the HPO_4^{2-} group. The peaks at 1461, 1420 and 869 cm^{-1} are attributed to the B–CO_3^{2-}, indicating the PO_4^{3-} substitution from the carbonate ions. The later signifies the presence of carbonated HA in those samples. It has been shown [43] that the velocity of H_3PO_4 addition into $Ca(OH)_2$ suspension affects the physical and chemical characteristics of BCP powders. Slow addition leads to higher amount of CO_3^{2-}, incorporated into the apatite structure. Consequently, the higher Ca/P molar ratio results in an increasing HA content of the calcinated BCP powders.

The chemical analysis (Table 2) of the supernatant solution, for the sample prepared without ageing, showed that the concentration of the phosphate and calcium ions in the supernatant were very low. Ageing of the slurry showed that phosphate concentration increased, while the calcium concentration increased in the first day and decreased the second. This observation indicates that the transformation of DCPD to HA takes place thought re-dissolution of precipitated DCPD. This finding is known as hardening mechanism of brushite cements [44]. During this procedure dissolution of the reactants occur leading to supersaturation of the solution (day 1). However once the ionic concentration reaches a critical limit, the nucleation of the new phase occurs, generally surrounding the powder particles and thus new phase keeps growing as the dissolution of the reagents continues. During the first hours the setting process is controlled by the dissolution kinetics of the raw materials, but once the new phase surrounds the reactants, the process is controlled by diffusion across the new phase [45].

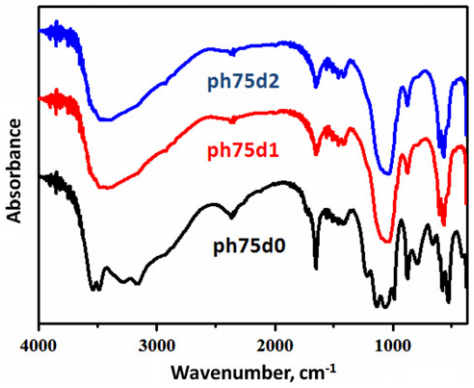

Fig. 4. FT-IR patterns of samples prepared in pH 7.5 without calcination.

Calcium and phosphorous contents of the resultant products were assayed by ICP-AES using spectrometer and determined using calibration curves. All the samples had Ca/P ratio higher than the theoretical of HA (Ca/P=1.667), which was increased as the ageing time increases. This observation is in accordance with the FT-IR results, and indicates that the precipitated HA was b-type carbonate hydroxyapatite (c-HA), due to the high concentration of carbonate ions in the supernatant.

Some researchers have shown that DCPD depending on conditions, can be stable, dissolve, or hydrolyze to hydroxyapatite (HA) [46]. The transformation of brushite to hydroxyapatite occurs via two stages; dissolution and precipitation [47]. An important factor affecting the rate of brushite dissolution is the concentration of calcium ions which decrease its solubility [48].

Fig. 5 depicts the TG/DTA curves of samples prepared in pH 7.5 with different ageing times. The overall mass loss of sample ph75d0 seems to be about double in value than samples ph75d1 and ph75d2, however the thermal decomposition of samples is almost same. As it can be seen from the TG curve of ph75d0 sample, mass loss seems to occur in 4 not distinguishable stages with yielding temperature at 900 °C. The first stage from ambient temperature to ~170 °C corresponds to the removal of moisture absorbed in the materials surface, as well as part of crystalline water (reaction 6), followed by the appearance of an endothermic tendency in the DTA curve. In this stage the mass loss is about 3%.

$$CaHPO_4 \cdot 2H_2O \rightarrow CaHPO_4 \cdot m(H_2O) + (2-m)H_2O \quad (6)$$

$$CaHPO_4 \cdot m(H_2O) \rightarrow CaHPO_4 + mH_2O \quad (7)$$

The highest amount of mass loss (~13.5%) occurs in the second stage between 170 and 370 °C and is attributed to the removal of the remained crystalline water (reaction 7). The corresponding mass loss of the samples ph75d1 and ph75d2 were ~5.5% and ~6.5% for the first stage and ~3.5% and 4% for the second one. This thermal behavior

Table 2
Chemical analysis of supernatant solutions.

Sample	Supernatant solution				Solid		
	Measured (ppm)		Calculated (mM)		Calculated (mgra)t		Ca/P
	P	Ca	HPO_4^-	Ca^{2+}	P	Ca	
Initial solution 200 mL			50.00	83.35			
pH75d0	1.00	0.27	0.032	0.007	9.988	16.697	1.672
pH75d1	16.07	9.43	0.519	0.235	9.800	16.609	1.695
pH75d2	34.69	3.21	1.120	0.080	9.569	16.669	1.742

indicates more adsorbed moisture and dramatically hydrolysis of DCPD after ageing of the slurry.

From this point forward the decomposition of brushite (reaction 3) and Ca-deficiency hydroxyapatite (reaction 5) to calcium pyrophosphate (CPP) take place into 3rd stage. This stage occurs between 370 and 550 °C accompanying a ~3% mass loss. For the sample ph75d0, the overall mass loss up to 550 °C was 19.5%, which is less than the pure DCPD (calculated mass loss 31.69%). The decrease in the removed water amount indicates the presence of other phases, such as HA and perhaps DCPA ($CaHPO_4$). The DCPA could be produced from the transformation of DCPD. The mass loss of 3rd stage of the samples ph75d1 and ph75d2 were ~1.5% due to the less amount of DCPD. Finally, in the 4th stage the reaction of HA with the CPP takes place (reactions 4 and 5).

In sample ph75d0 at about 580 °C an exothermic weak peak in the DTA curve, is attributed to the transformation of the amorphous CPP to the crystalline γ-CPP. The peak depicted in the DTA curve above 1300 °C is attributed to the melting of the CPP.

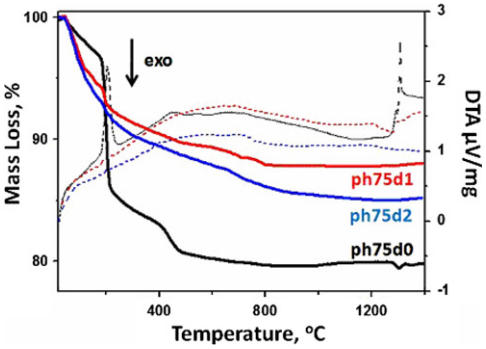

Fig. 5. TG/DTA curves of the raw materials prepared in pH 7.5.

SEM images of both raw and calcined samples are depicted in Figs. 6 and 7. Samples prepared in 900 °C show different structure than raw materials. Sample prepared without ageing (ph75d0, Fig. 6a) is a biphasic DCPD/HA material which seems to be consisted from lathlike particles, as substrate, which are overlapped with spheroid and rod like particles of HA. It is known that synthetic brushite powders mostly exhibit large tabular, lathlike, or rectangular prismatic particles [49]. Sample ph75d1 (Fig. 6b) show interconnected particles full of wrinkles, while the sample ph75d2 (Fig. 6c) flake-like particles. Those findings are in accordance to previous proposed mechanisms [50,51] it has been shown that needle- like crystals are obtained when fine powder is used as the initial high crystalline DCPD/HA material, whereas plate-like crystals are obtained using coarser powder such as the low crystalline HA samples prepared after ageing.

Calcined samples (Fig. 7) have typical morphology for sintered calcium phosphate materials. Samples cph75d0 and cph75d1 are compact with parallel stripes on their surface, which are probably formed by the interaction of the lathe-like DCPD and rod like HA particles. On the contrary sample cph75d2 has a sponge-like structure.

The crystal morphologies depend on the correlation between the driving force of crystallization and the diffusion of atoms, ions, molecules, or heat the control of nucleation and morphology on aqueous solution-based crystal growth. Such control can be achieved by adjusting the pH in the initial process or the ageing time of the slurry. The results show that pH value is a significant parameter in altering the calcium phosphate particle morphology. The conversion of DCPD to HA, is strongly

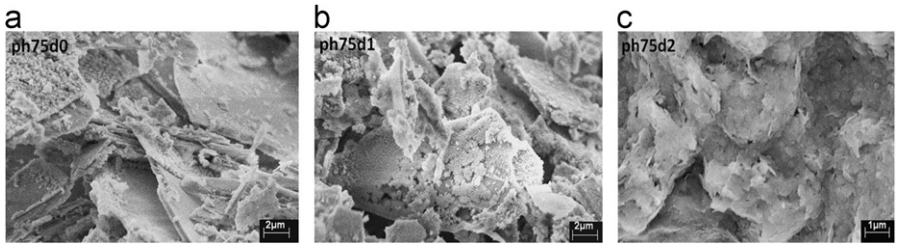

Fig. 6. SEM images of raw samples prepared in pH 7.5 without ageing (a), after 1 day (b) and after 2 day (c).

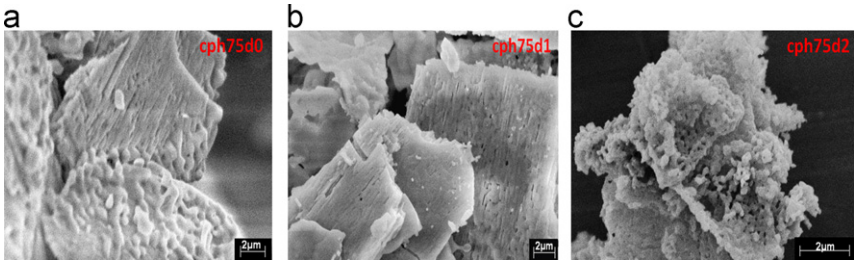

Fig. 7. SEM images of calcined samples prepared in pH 7.5 without ageing (a), after 1 day (b) and after 2 day (c).

depended on the incongruent dissolution of DCPD, which occurs during the ageing of the slurry, under the above mentioned conditions. The later could lead, depending on the ageing time and/or calcination, to the formation either β-TCP or HA.

4. Conclusion

The preparation of biphasic DCPD/HA materials via hydrolysis precipitation method is strongly depended on the starting material formed. Physiological pH values favor the production of biphasic DCPD/HA materials, while ageing time favors the production of low crystalline carbonated HA through hydrolysis. Calcination of the sample prepared after two days ageing time seems to increase HA crystallinity. After calcinations TCP and/or CPP crystalline phases were produced according to the composition of the BCP raw materials. The textural properties, of both raw and calcined samples, are also strongly depended on the ageing time. Ageing time of clinical interest (2 days time) seems to promote BCPs which have been reported for their conductivity to cell interactions that balance osteoclastic and osteoblastic activity. Orthophosphate materials such as TCP-based BCPs exhibit high degree of solubility and biodegradability supporting osteoblastic cellular proliferation and differentiation while apatitic materials are more stable resulting materials degradation attributed to osteoclastic attachments. The obtained variety of calcium phosphate materials has been achieved simply by adjusting the ageing time and the calcination temperature of the initial produced slurry under physiological conditions. The hydrolysis/precipitation method can be applied in bioceramics technology in order to produce materials with desirable properties under physiological pH for further in vitro studies.

References

[1] A. Wang, D. Liu, H. Yin, H. Wu, Y. Wada, M. Ren, T. Jiang, X. Cheng, Y. Xu, Size-controlled synthesis of hydroxyapatite nanorods by chemical precipitation in the presence of organic modifiers, Materials Science and Engineering C 27 (4) (2007) 865–869.

[2] Y. Han, S. Li, X. Wang, X. Chen, Synthesis and sintering of nanocrystalline hydroxyapatite powders by citric acid sol–gel combustion method, Materials Research Bulletin 39 (1) (2004) 25–32.

[3] J. Liu, K. Li, H. Wang, M. Zhu, H. Yan, Rapid formation of hydroxyapatite nanostructures by microwave irradiation, Chemical Physical Letters 396 (4–6) (2004) 429–432.

[4] G. Guo, Z. Wang, H. Guo, Preparation of hydroxyapatite nanoparticles by reverse microemulsion, Ceramic International 31 (6) (2005) 869–872.

[5] A. Milev, G.S.K. Kannangara, B. Ben-Nissan, Morphological stability of hydroxyapatite precursor, Materials Letters 57 (13–14) (2003) 1960–1965.

[6] R.Z. LeGeros, J.P. LeGeros, Dense hydroxyapatite, in: L.L. Hench, J. Wilson (Eds.), An Introduction to Bioceramics, World Scientific, Singapore, 1993.

[7] T. Yamamuro, L.L. Hench, J. Wilson, Handbook of Bioactive Ceramics Vol II Calcium Phosphate and Hydroxyapatite Ceramics, CRC Press, Boca Raton, Florida USA, 1990.

[8] W. Suchanek, M. Yoshimura, Processing and properties of Hap-based biomaterials for use as hard tissue replacement implants, Journal of Materials Research 13 (1) (1998) 94.

[9] S.H. Maxian, J.P. Zawadsky, M.G. Dunn, Mechanical and histological evaluation of amorphous calcium phosphate and poorly crystallized hydroxyapatite coatings on titanium implants, Journal of Biomedical Materials Research Part A 27 (6) (1993) 717–728.

[10] C.A. Van Blitterswijk, Y.P. Bovell, J.S. Flach, H. Leenders, I. van den Brink, J. de Bruijn, Variations in hydroxylapatite crystallinity: effect on interface reactions, in: R.G.T. Geesink, M.T. Manley (Eds.), Hydroxylapatite Coatings in Orthopaedic Surgery, Raven Press, New York, 1993, pp. 33–47.

[11] K.A. Gross, C.C. Berndt, D.D. Goldschlag, V.J. Iacono, In vitro changes on hydroxyapatite coatings, International Journal of Oral Maxillofacial Implants 12 (5) (1997) 589–597.

[12] J.M. Kuemmerle, A. Oberle, C. Oechslin, M. Bohner, C. Frei, I. Boecken, et al., Assessment of the suitability of a new brushite calcium phosphatecement for cranioplasty—an experimental study in sheep, Journal of Craniomaxillofacial Surgery 33 (1) (2005) 37–44.

[13] F.C. Driessens, J.A. Planell, M.G. Boltong, I. Khairoun, M.P. Ginebra, Osteotransductive bone cements, Proceedings of the Institution of Mechanical Engineers H 212 (6) (1998) 427–435.

[14] R.O. Oreffo, F.C. Driessens, J.A. Planell, J.T. Triffitt, Effects of novel calcium phosphate cements on human bone marrow fibroblastic cells, Tissue Engineering 4 (3) (1998) 293–303.

[15] M. Banu, X. Ranz, S. Somrani, A. Tofighi, C. Combes, C. Rey, Amorphous calcium-phosphate and biomimetic materials, in: A. Ravaglioli, A. Krajewski, editors, Proceedings of the 7th cells ceramics and tissues, ISTEC-CNR Faenza, Tipo-Litografia Fabbri (Modigliana), 13–15 June 2001, pp. 161–168.

[16] R.Z. LeGeros, S. Lin, R. Rohanizadeh, D. Mijares, J.P. Legeros, Biphasic calcium phosphate bioceramics: preparation, properties and applications, Journal of Materials Science: Materials in Medicine 14 (3) (2003) 201–209.

[17] F. Barrere, C.A. van Blitterswijk, K. de Groot, Bone regeneration: molecular and cellular interactions with calcium phosphate ceramics, International Journal of Nanomedicine 1 (3) (2006) 317–332.

[18] R.Z. LeGeros, G. Daculsi, In vivo transformation of biphasic calcium phosphate ceramics: ultrastructural and physico–chemical characterizations,, in: T. Yamamuro, J. Wilson-Hench (Eds.), Handbook of Bioactive Ceramics, 11, CRC Press, Boca Raton, Fla, USA,, 1997, pp. 17–28.

[19] D. Arcos, I. Izquierdo-Barba, M. Vallet-Regí, Promising trends of bioceramics in the biomaterials field, Journal of Materials Science: Materials in Medicine 20 (2) (2009) 447–455.

[20] R. Xin, Y. Leng, J. Chen, Q. Zhang, A comparative study of calcium phosphate formation on bioceramics in vitro and in vivo, Biomaterials 26 (33) (2005) 6477–6486.

[21] Y.R. Duan, Z.R. Zhang, C.Y. Wang, J.Y. Chen, X.D. Zhang, Dynamic study of calcium phosphate formation on porous HA/TCP ceramics, Journal of Materials Science: Materials in Medicine 15 (11) (2004) 1205–1211.

[22] E. Spassova, S. Gintenreiter, E. Halwax, D. Moser, C. Schopper, R. Ewers, Chemistry, ultrastructure and porosity of monophasic and biphasic bone forming materials derived from marine algae, Materialwissenschaff und Werkstofftechnik 38 (12) (2007) 1027–1034.

[23] R. Emadi, S.I. Roohani Esfahani, F. Tavangarian, A novel, low temperature method for the preparation of b-TCP/HAP biphasic nanostructured ceramic scaffold from natural cancellous bone, Materials Letters 64 (8) (2010) 993–996.

[24] Pankaj Sarin, Sang-Jin Lee, Zlatomir D. Apostolov, Waltraud M. Kriven, Porous biphasic calcium phosphate scaffolds from cuttlefish bone, Journal of the American Ceramic Society 94 (8) (2011) 2362–2370.

[25] D.L. Alge, G. Santa Cruz, W.S. Goebel, T.-M.G. Chu, Characterization of dicalcium phosphate dihydrate cements prepared using a

novel hydroxyapatite-based formulation, Biomedical Materials 4 (2009) 025016.
[26] H.H.T. Hsu, B.G. Abb, Role of bicarbonate/CO_2 buffer in the initiation of vesicle-mediated calcification: mechanisms of aortic calcification related to atherosclerosis, Biochimica et Biophysica Acta (1690).
[27] Y. Ramaswamy, D.R. Haynes, G. Berger, R. Gildenhaar, H. Lucas, C. Holding, H. Zreiqat, Bioceramics composition modulate resorption of human osteoclasts, Journal of Material Science: Materials in Medicine 16 (2005) 1199–1205.
[28] L.L. Hench, Biomaterials: a forecast for the future, Biomaterials 16 (1998) 1419–1423.
[29] C. Ohtsuki, T. Kokubo, M. Neo, S. Kotani, T. Yamamuro, et al., Bone bonding mechanism of sintered $3CaO–P_2O_5$, Phosphate Research Bulletin 1 (1991) 191–196.
[30] S. Kotani, Y. Fujita, T. Kitsugi, T. Nakamura, T. Yamamuro, C. Ohtsuki, et al., Bone bonding mechanism of beta-tricalcium phosphate, Journal of Biomedical Materials Research 10 (1991) 1303–1315.
[31] H.M. Kim, T. Himeno, M. Kawashita, T. Kokubo, T. Nakamura, The mechanism of biomineralization of bone-like apatite on synthetic hydroxyapatite: an in vitro assessment, Journal of the Royal Society Interface 1 (2004) 17–22.
[32] A. Ramila, S. Padila, B. Munoz, M. Vallet-Regi, A new hydroxyapatite/glass biphasic material: in vitro bioactivity, Chemistry of Materials 14 (2002) 2439–2443.
[33] F. Balas, J. Perez-Pariente, M. Vallet-Regi, In vitro bioactivity of silicon substituted hydroxyapatites, Journal of Biomedical Materials Research A 66 (2003) 364–375.
[34] R. Xin, Y. Leng, J. Chen, Q. Zhang, A comparative study of calcium phosphate formation on bioceramics in vitro and in vivo, Biomaterials 26 (2005) 6477–6486.
[35] G.C. Koumoulidis, T.C. Vaimakis, A.T. Sdoukos, N.K. Boukos, C.C. Trapalis, Preparation of lathlike particles using high speed dispersing equipment, Journal of the American Ceramic Society 84 (2001) 1203–1208.
[36] M.-P. Ginebra, C. Canal, M. Espanol, D. Pastorino, E.B. Montufar, Calcium phosphate cements as drug delivery materials, Advanced Drug Delivery Reviews (2012)http://dx.doi.org/10.1016/j.addr.2012.01.008.
[37] L. Grover, J. Knowles, G. Fleming, J. Barralet, In vitro ageing of brushite calcium phosphate cement, Biomaterials 24 (2003) 4133–4141 1406.
[38] F. Theiss, D. Apelt, B. Brand, A. Kutter, K. Zlinszky, M. Bohner, et al., Biocompatibility and resorption of a brushite calcium phosphate cement, Biomaterials 26 (2005) 4383–4394.
[39] E.P. Frankenburg, S.A. Goldstein, T.W. Bauer, S.A. Harris, R.D. Poser, Biomechanical and histological evaluation of a calcium phosphate cement, Journal of Bone and Joint Surgery 80 (1998) 1112–1124.
[40] S. Wenisch, J.P. Stahl, U. Horas, C. Heiss, O. Kilian, K. Trinkaus, et al., In vivo mechanisms of hydroxyapatite ceramic degradation by osteoclasts: fine structural microscopy, Journal of Biomedical Materials Research A 67 (2003) 713–718.
[41] M. Siebbers, P. Brugge, X. Walboomers, J. Jansen, Integrins as linker proteins between osteoblasts and bone replacing materials. A critical review, Biomaterials 26, 2005, 137–146.
[42] T.L. Arinzeh, T. Tran, J. Mcalary, G. Daculsi, A comparative study of biphasic calcium phosphate ceramics for human mesenchymal stem-cell-induced bone formation, Biomaterials 17 (2005) 3631–3638.
[43] J. Marchi, Influence of synthesis conditions on the characteristics of biphasic calcium phosphate powders, International Journal of Applied Ceramic Technology 6 (2009) 60–71.
[44] W.C. Chen, J.H.C. Lin, C.P. Ju, Transmission electron microscopic study on setting mechanism of tetracalcium phosphate/dicalcium phosphate anhydrous-based calcium phosphate cement, Journal of Biomedical Materials Research A 64 (2003) 664–671.
[45] M.P. Ginebra, E. Fernandez, F.C.M. Driessens, J.A. Planell, Modeling of the hydrolysis of alpha-tricalcium phosphate, Journal of the American Ceramic Society 82 (1999) 2808–2812.
[46] B.R. Constantz, B.M. Barr, I.C. Ison, M.T. Fulmer, J. Baker, L. McKinney, S.B. Goodman, S. Gunasekaren, D.C. Delaney, J. Ross, R.D. Poser, Histological, chemical, and crystallographic analysis of four calcium phosphate cements in different rabbit osseus sites, Journal of Biomedical Materials Research Part B: Applied Biomaterials 43 (4) (1998) 451–461.
[47] J. Xie, C. Riley, K. Chittur, Effect of albumin on brushite transformation to hydroxyapatite, Journal of Biomedical Materials Research 57 (3) (2001) 357–365.
[48] M. Kumar, H. Dasarathy, C. Riley, Electrodeposition of brushite coatings and their transformation to hydroxyapatite in aqueous solutions, Journal of Biomedicine Materials Research Part B 45 (4) (1999) 302–310.
[49] A.C. Tas, Monetite ($CaHPO_4$) synthesis in ethanol at room temperature, Journal of the American Ceramic Society 92 (12) (2009) 2907–2912.
[50] M. Espanol, R.A. Perez, E.B. Montufar, C. Marichal, A. Sacco, M.P. Ginebra, Intrinsic porosity of calcium phosphate cements and its significance for drug delivery and tissue engineering applications, Acta Biomaterialia 5 (2009) 2752–2762.
[51] M.P. Ginebra, F. Driessens, J.A. Planell, Effect of the particle size on the micro and nanostructural features of a calcium phosphate cement: a kinetic analysis, Biomaterials 25 (2004) 3453–3462.